




Commensal Microbiota Effects on Craniofacial Skeletal Growth and Morphology

Joy E. Gerasco,^{1,2,3,4}  Jessica D. Hathaway-Schrader,^{1,2,3} Nicole A. Poulides,^{1,2,3} Matthew D. Carson,^{1,2,3} Naoto Okhura,⁵ Caroline Westwater,^{1,6} Nan E. Hatch,⁵  and Chad M. Novince^{1,2,3} 

¹Department of Oral Health Sciences, College of Dental Medicine, Medical University of South Carolina, Charleston, SC, USA

²Department of Stomatology-Division of Periodontics, College of Dental Medicine, Medical University of South Carolina, Charleston, SC, USA

³Department of Pediatrics-Division of Endocrinology, College of Medicine, Medical University of South Carolina, Charleston, SC, USA

⁴Department of Orthodontics, Adam's School of Dentistry, University of North Carolina, Chapel Hill, NC, USA

⁵Department of Orthodontics and Pediatric Dentistry, School of Dentistry, University of Michigan, Ann Arbor, MI, USA

⁶Department of Microbiology and Immunology, College of Medicine, Medical University of South Carolina, Charleston, SC, USA

ABSTRACT

Microbes colonize anatomical sites in health to form commensal microbial communities (e.g., commensal gut microbiota, commensal skin microbiota, commensal oral microbiota). Commensal microbiota has indirect effects on host growth and maturation through interactions with the host immune system. The commensal microbiota was recently introduced as a novel regulator of skeletal growth and morphology at noncraniofacial sites. Further, we and others have shown that commensal gut microbes, such as segmented filamentous bacteria (SFB), contribute to noncraniofacial skeletal growth and maturation. However, commensal microbiota effects on craniofacial skeletal growth and morphology are unclear. To determine the commensal microbiota's role in craniofacial skeletal growth and morphology, we performed craniometric and bone mineral density analyses on skulls from 9-week-old female C57BL/6T germ-free (GF) mice (no microbes), excluded-flora (EF) specific-pathogen-free mice (commensal microbiota), and murine-pathogen-free (MPF) specific-pathogen-free mice (commensal microbiota with SFB). Investigations comparing EF and GF mice revealed that commensal microbiota impacted the size and shape of the craniofacial skeleton. EF versus GF mice exhibited an elongated gross skull length. Cranial bone length analyses normalized to skull length showed that EF versus GF mice had enhanced frontal bone length and reduced cranial base length. The shortened cranial base in EF mice was attributed to decreased presphenoid, basisphenoid, and basioccipital bone lengths. Investigations comparing MPF mice and EF mice demonstrated that commensal gut microbes played a role in craniofacial skeletal morphology. Cranial bone length analyses normalized to skull length showed that MPF versus EF mice had reduced frontal bone length and increased cranial base length. The elongated cranial base in MPF mice was due to enhanced presphenoid bone length. This work, which introduces the commensal microbiota as a contributor to craniofacial skeletal growth, underscores that noninvasive interventions in the gut microbiome could potentially be employed to modify craniofacial skeletal morphology. © 2023 The Authors. *JBMR Plus* published by Wiley Periodicals LLC on behalf of American Society for Bone and Mineral Research.

KEY WORDS: BONE-MICROBIOTA INTERACTORS; CRANIOMETRY; PRECLINICAL STUDIES

Introduction

Nonpathogenic microbes colonize host anatomic barrier sites to form commensal microbiota communities (e.g., commensal gut microbiota, commensal skin microbiota, commensal oral microbiota).^[1–4] Commensal microbiota interactions with the host direct the development of immunity, which has indirect effects on host growth and maturation.^[5–8] The

commensal microbiota was recently introduced as a critical regulator of skeletal growth and morphology at noncraniofacial sites.^[9–14] Moreover, our group and others have shown that commensal gut microbes, such as segmented filamentous bacteria (SFB), contribute to noncraniofacial skeletal growth and maturation.^[13,14]

The craniofacial skeleton is a unique skeletal complex that derives from the neural crest and mesoderm and develops

This is an open access article under the terms of the [Creative Commons Attribution](#) License, which permits use, distribution and reproduction in any medium, provided the original work is properly cited.

Received in original form February 1, 2023; revised form May 7, 2023; accepted May 11, 2023.

Address correspondence to: Chad M. Novince, Department of Oral Health Sciences, Medical University of South Carolina, 173 Ashley Avenue, Charleston, SC 29425, USA.

Email: novincec@musc.edu

Additional supporting information may be found online in the Supporting Information section.

JBMR[®] Plus (WOA), Vol. 7, No. 8, August 2023, e10775.

DOI: 10.1002/jbm4.10775

© 2023 The Authors. *JBMR Plus* published by Wiley Periodicals LLC. on behalf of American Society for Bone and Mineral Research.

through both intramembranous and endochondral ossification.^[15,16] The craniofacial skeleton houses the brain and sensory organs for vision, hearing, taste, and smell, supports mastication and speaking, and impacts appearance and psychosocial well-being. Therefore, mechanisms regulating craniofacial growth and morphology are important.^[17,18] Murine models have been extensively used to study normal craniofacial development^[19–21] and craniofacial malformations caused by genetics, teratogens, and environmental factors.^[22–24] However, the role of commensal microbiota in physiologic craniofacial skeletal growth and morphology is unknown.

To define the role of commensal microbiota in normal craniofacial skeletal growth and morphology, we performed studies comparing germ-free (GF) mice, excluded-flora (EF) mice, and murine-pathogen-free (MPF) mice. GF mice, which are devoid of all microbes, are reared in sterile isolators. Specific-pathogen-free mice, which are colonized by commensal microbiota, are reared in ventilated isolators within barrier facilities that validate specific microbes are not present. Taconic Biosciences animal health barrier facilities provided the opportunity to acquire specific-pathogen-free mice that differed by the known colonization status of SFB. EF mice are specific-pathogen-free mice that are devoid of SFB, and MPF mice are specific-pathogen-free mice that harbor SFB. SFB are commensal gut bacteria that colonize the ileum following weaning.^[25–27] SFB colonization critically influences commensal microbiota actions on host immunity and development.^[13,14,27–30] Therefore, comparing specific-pathogen-free mice that differ by SFB colonization status provides insights about the role of commensal gut microbes in commensal microbiota effects on normal growth and morphology.

Cephalometric and craniometric measurements are used in the surgical and dentofacial orthopedic treatment of craniofacial malformations and achieve a more harmonious dentofacial complex.^[31,32] Craniometry is utilized in preclinical murine model research to advance knowledge about abnormal and healthy craniofacial skeletal growth and development.^[19–24] Herein, we performed craniometric and bone mineral density (BMD) analyses in skulls from 9-week-old female C57BL/6T GF mice (no microbes), EF mice (commensal microbiota), and MPF mice (commensal microbiota with SFB). Comparing GF mice to EF mice help define the role of commensal microbiota in normal craniofacial skeletal growth and morphology. Comparing EF mice to MPF mice made it possible to discern commensal gut microbe contributions to physiologic craniofacial skeletal growth and morphology.

Materials and Methods

Mice

C57BL/6T GF mice were obtained from Taconic Biosciences (Rensselaer, NY, USA) and were bred and maintained in sterile isolators at the Medical University of South Carolina (MUSC; Charleston, SC, USA) Gnotobiotic Animal Core. GF mice were fed autoclaved LabDiet 5010 (LabDiet, St. Louis, MO, USA). Nine-week-old EF mice and MPF mice were obtained from Taconic Biosciences (Rensselaer, NY, USA), where they were bred and maintained in their respective barrier facilities. EF and MPF mice were fed autoclaved NIH-31M diet (Envigo, Indianapolis, IN, USA). Upon arrival at MUSC, the EF and MPF mice were housed in a specific-pathogen-free vivarium and sacrificed within 48 h. All animals were euthanized at 9.0–9.5 weeks of age. Animals were group-housed four to five per cage. Room temperature and

humidity were maintained within the ranges recommended by the *Guide for the Care and Use of Laboratory Animals*.^[33] Room light:dark cycle was maintained on a 12-h on:off schedule. Animal experimentation was approved by the MUSC Institutional Animal Care and Use Committee and carried out in accordance with approved guidelines.

Quantitative real-time PCR (qRT-PCR) 16S rDNA analyses

Following euthanasia, ileum contents were collected for bacterial 16S rDNA analysis. Genomic DNA was isolated using Qiagen DNeasy Powersoil Pro Kit (Qiagen, Hilden, Germany), per the manufacturer's instructions. Total DNA was quantified using the Nanodrop 1000 (Thermo Fisher Scientific, Waltham, MA, USA). 16S rDNA was amplified on the StepOnePlus System (Applied Biosystems, Foster City, CA, USA) via a qRT-PCR reaction protocol using 2× Fast SYBR Green Master Mix (Applied Biosystems) forward/reverse primers (Integrated DNA Technology, Coralville, IA, USA) and DNA template, as described previously.^[34–36] A 30-cycle qRT-PCR protocol was utilized; cycle number 25 was the cutoff for nonspecific amplification of the Universal 16S gene.^[13,37] Bacterial load analysis was conducted in which bacterial load was evaluated by normalizing the Universal 16S gene to a bacterial DNA standard (ZymoBIOMICS; Zymo Research, Irvine, CA, USA), as described previously.^[13, 36, 38] Relative quantification of Universal 16S rDNA was carried out by the $2^{-\Delta CT}$ method.^[39] In the bacterial phyla analysis, phylum-level outcomes are reported relative to the Universal 16S gene, as described previously.^[36, 38] Relative quantification of phylum-level rDNA was performed by the $2^{-\Delta\Delta CT}$ method.^[40] In SFB analysis, SFB presence was evaluated by normalizing the SFB rDNA gene to a bacterial DNA standard (ZymoBIOMICS; Zymo Research), as described previously.^[13, 41] Relative quantification of SFB rDNA was performed by the $2^{-\Delta CT}$ method.^[39] Integrated DNA Technologies forward (F)/reverse (R) primer sequences included the following:

Universal 16S^[34]: F = 5'-AAACTCAAAGAATTGACGG-3'; R = 5'-CTCACRRACAGAGCTGAC-3',
Pseudomonadota^[34]: F = 5'-TCGTCAGCTCGTGTGTGA-3'; R = 5'-CGTAAGGGCCATGATG-3',
Actinomycetota^[34]: F = 5'-TACGGCCGCAAGGCTA-3'; R = 5'-TCRTCCCCACCTTCTCCG-3',
Bacteroidota^[34]: F = 5'-CRAACAGGATTAGATACCCT-3'; R = 5'-GGTAAGGTTCTCGCGTAT-3',
Bacillota^[34]: F = 5'-TGAAACTYAAAGGAATTGACG-3'; R = 5'-ACCATGCACCACCTGTC-3',
SFB^[13, 41]: F = 5'-GACGCTGAGGCATGAGAGCAT-3'; R = 5'-GACGGCAGGATTGTTATCA-3'.

qRT-PCR mRNA analyses

Ileum specimens were flash-frozen, pulverized, and homogenized in TRIzol Reagent (Invitrogen, Carlsbad, CA, USA). RNA extraction was performed via the TRIzol method, as reported previously.^[13, 41] Total RNA was quantified via the NanoDrop 1000 (Thermo Fisher Scientific). cDNA was synthesized from RNA using Taqman Random Hexamers and Reverse Transcription Reagents (Applied Biosystems), following the manufacturer's protocol.^[13, 41] mRNA was amplified on the StepOnePlus System (Applied Biosystems) via a qRT-PCR reaction protocol using TaqMan Fast Advanced Master Mix and primer probes (Applied Biosystems), as described previously.^[13, 41] Relative quantification of mRNA was performed by the $2^{-\Delta\Delta CT}$ method^[40]; *Gapdh* was

used as an internal control gene. The TaqMan primer-probe assays used included *Gapdh* = Mm99999915_g1; *Il17a* = Mm00439618_m1.

Tibia microradiography imaging/length analysis

Following euthanasia, tibiae were isolated and fixed in 10% phosphate-buffered formalin for 24 h at room temperature; specimens were stored in 70% ethanol at 4°C. Ex vivo microradiographs of tibiae were acquired with a Faxitron LX-60 (Faxitron X-ray, Lincolnshire, IL, USA), using the following acquisition parameters: beam energy = 36 kVp, exposure time = 40 s. Tibia length measurements were performed via calibrated microradiograph images, measuring from the intercondylar eminence to the lateral malleolus.

Skull micro-CT imaging

Following euthanasia, skulls were isolated and fixed in 10% phosphate-buffered formalin for 24 h at room temperature; specimens were stored in 70% ethanol at 4°C. Mandibles were dissected and skull specimens were scanned with a Scanco Medical micro-CT (μ CT) 40 scanner (Scanco Medical; Brüttisellen, Switzerland), using the following acquisition parameters: X-ray tube potential = 70 kVp, X-ray intensity = 55 μ A, integration time = 200 ms, and isotropic voxel size = 18 μ m³. Calibrated three-dimensional (3D) images of skulls were reconstructed for craniometric measurements and BMD analyses.

μ CT craniometric analyses

Skull craniometric measurements were performed using Analyze 14.0 Bone Microarchitecture Analysis software (Analyze Direct, Seattle, WA, USA). Linear measurements were carried out on reoriented 3D μ CT reconstructions, with a fixed threshold of 2500 Hounsfield units (HU). For frontal and parietal bones, linear measurements were taken bilaterally and averaged. Linear measurements were performed three separate times for each outcome of interest, and the arithmetic mean of these measurements is reported for each biological replicate. Skull length (nasale to pario) is reported as a direct measurement. All other linear measurements were normalized to skull length (nasale to pario) to account for skull size differences, as reported previously.^[42–44] Landmarks for craniometric analyses are depicted via schematics: skull length, skull width, and skull height (Fig. S1); skull length, nasal bone length, cranial vault bone lengths, and cranial base bone lengths (Fig. S1). Studies were performed and are reported in accordance with guidelines for assessment of bone microstructure in rodents using μ CT.^[45]

μ CT bone mineral density analyses

Skull BMD measurements were acquired using Analyze 14.0 Bone Microarchitecture Analysis software (Analyze Direct). BMD analyses were carried out using reoriented 3D μ CT reconstructions. A fixed threshold of 2000 HU was used to discern mineralized tissue. BMD analysis was performed in the following volumes of interest, adapted from methods described previously.^[21, 46, 47] *Basioccipital bone analysis*: 900 μ m³ volume of interest (VOI) positioned 180 μ m posterior to the junction of the basisphenoid and basioccipital bones, the spheno-occipital synchondrosis (SOS). The VOI was centered mediolaterally across the median sagittal plane. *Basisphenoid bone analysis*: 900 μ m³ VOI positioned 360 μ m anterior to the SOS and 360 μ m superior

from the inferior extent of the pterygoid bone/process at the intersection of the SOS. *Presphenoid bone analysis*: 900 μ m³ VOI positioned 270 μ m anterior to the junction of the basisphenoid and presphenoid bones, the intersphenoid synchondrosis (ISS). The VOI was oriented in the superior–inferior and mediolateral directions centered on the presphenoid bone. *Frontal bone analysis*: 1440 μ m³ VOI was analyzed at the left frontal bone. The VOI was positioned 720 μ m lateral to the sagittal suture and 1440 μ m anterior to the coronal suture. *Parietal bone analysis*: 1440 μ m³ VOI was analyzed at the left parietal bone. The VOI was positioned 1440 μ m lateral to the sagittal suture and centered between the lambdoid and coronal sutures in the anterior–posterior plane. *Interparietal bone analysis*: 900 μ m³ VOI positioned 900 μ m anterior to the junction of the interparietal and occipital bones. The VOI was centered mediolaterally across the median sagittal plane. Landmarks and VOIs for BMD analysis are depicted via schematics: cranial vault bones (Fig. S2A) and cranial base bones (Fig. S2E). Studies were performed and are reported in accordance with guidelines for assessment of bone microstructure in rodents using μ CT.^[45]

Statistical analysis

Statistical analysis was carried out using GraphPad Prism version 9.0 (GraphPad, La Jolla, CA, USA). Unpaired two-tailed *t*-test ($p < 0.05$) was performed comparing 16S rDNA analysis outcomes in EF versus MPF mice. One-way ANOVA ($\alpha = 0.05$) with Tukey post hoc test ($p < 0.05$) was carried out comparing outcomes in GF, EF, and MPF mice for all other studies. When unpaired *t* test was used, *F* test was performed to validate the data come from populations that are Gaussian and have equal variances. When one-way ANOVA was utilized, a Brown–Forsythe test and Levene test were carried out to validate the data come from populations that are Gaussian and have equal variances. The Shapiro–Wilk test ($\alpha = 0.05$) was applied to all data sets to determine whether the data came from normally distributed populations. In the case that the Shapiro–Wilk test did not validate that a data set was normally distributed, the ROUT outlier test ($Q = 0.1\%$) was performed to remove definitive outliers. Data are plotted as box and whisker plots that display all data points, the interquartile range (height of the box), median (internal horizontal bar), arithmetic mean (“plus” sign), and maximum and minimum values (external upper and lower bars). Power analysis was performed based on the authors’ prior experience investigating skeletal morphology in mice and was carried out in consultation with the MUSC Bioinformatics Core Biostatistical Unit.

Results

Commensal microbiota does not alter somatic growth in 9-week-old female C57BL/6T mice

We compared 9-week-old female C57BL/6T GF mice (no microbes) and EF mice (commensal microbiota) to determine the role of commensal microbiota in craniofacial skeletal growth and morphology (Fig. 1A). We compared 9-week-old female C57BL/6T EF mice (commensal microbiota) and MPF mice (commensal microbiota with SFB) to delineate whether commensal gut microbes contributed to commensal microbiota effects on craniofacial skeletal growth and morphology (Fig. 1A).

16S rDNA analyses were performed with ileum contents to validate the murine gut microbiome phenotype (Fig. 1B–D).

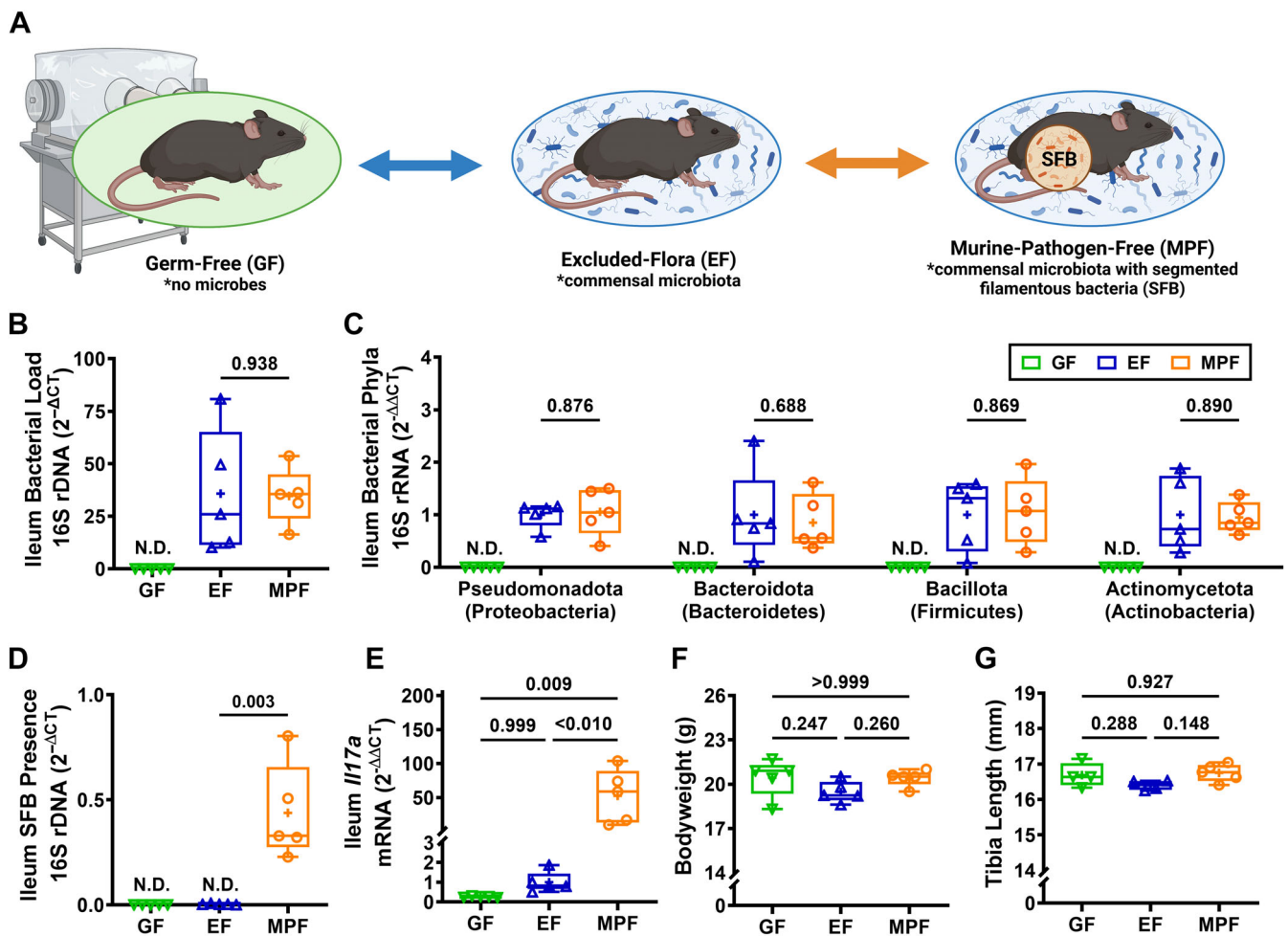


Fig. 1. Commensal microbiota do not alter somatic growth in 9-week-old female C57BL/6T mice. (A) Female C57BL/6T GF mice (no microbes), EF mice (commensal microbiota), and MPF mice (commensal microbiota with SFB) were euthanized at age 9 weeks; specimens were isolated for analyses. (A) Schematic of study design. (B–D) qRT-PCR 16S rDNA analysis of ileum contents ($n = 5/\text{group}$) evaluating (B) bacterial load, (C) phyla, and (D) SFB presence. (B) Bacterial load determined by normalizing the Universal 16S gene to a bacterial DNA standard; quantification via the $2^{-\Delta\Delta CT}$ method. (C) Phylum outcomes determined by normalizing phylum 16S genes to the Universal 16S gene; quantification by the $2^{-\Delta\Delta CT}$ method. (D) SFB presence determined by normalizing the SFB 16S gene to a bacterial DNA standard; quantification via the $2^{-\Delta\Delta CT}$ method. (E) qRT-PCR mRNA analysis of *Il17a* in ileum ($n = 5/\text{group}$); relative quantification of mRNA was performed via the $2^{-\Delta\Delta CT}$ method. (F) Body weight analysis ($n = 5/\text{group}$). (G) Tibia length analysis ($n = 4\text{--}5/\text{group}$). (B–D) Unpaired two-tailed t -test (p value < 0.05) was performed comparing 16S rDNA analysis outcomes in EF versus MPF mice. (E, F) One-way ANOVA ($\alpha = 0.05$) with Tukey post hoc test (p value < 0.05) was carried out comparing outcomes in GF, EF, and MPF mice.

Bacteria were not detectable in GF mice (Fig. 1B–D). The bacterial load was similar (Fig. 1B) and bacterial phyla expression was not different (Fig. 1C) in EF versus MPF mice. SFB was detected in MPF mice, but not EF mice (Fig. 1D). Consistent with the presence of SFB, which induces $T_H17/IL17A$ immunity,^[27, 28] *Il17a* mRNA was greater than 50 times higher in the ileum of MPF versus EF mice (Fig. 1E).

We evaluated alterations in body weight and tibia length to determine commensal microbiota effects on somatic (body) growth outcomes. Body weight measurements were performed immediately prior to euthanasia. Tibia length measurements were carried out on ex vivo microradiographs of tibiae. Body weight was similar (Fig. 1F) and tibia length was not different (Fig. 1G) in GF versus EF mice or EF versus MPF mice. These data support the idea that commensal microbiota

does not alter somatic growth outcomes in 9-week-old female C57BL/6T mice.

Commensal microbiota impacts craniofacial skeletal morphology in 9-week-old female C57BL/6T mice

We performed craniometric measurements on reconstructed 3D μ CT images of skulls to evaluate commensal microbiota effects on craniofacial skeletal growth and morphology (Figs. 2 and S1). Skull length (Fig. 2A) is reported as a direct measurement. Skull width (Fig. 2B), skull height (Fig. 2C), nasal bone length (Fig. 2D), cranial vault bone lengths (Fig. 2E–H), and cranial base bone lengths (Fig. 2I–L) are reported relative to skull length.

The direct skull length was increased in EF versus GF mice (Fig. 2A), which demonstrates that commensal microbes

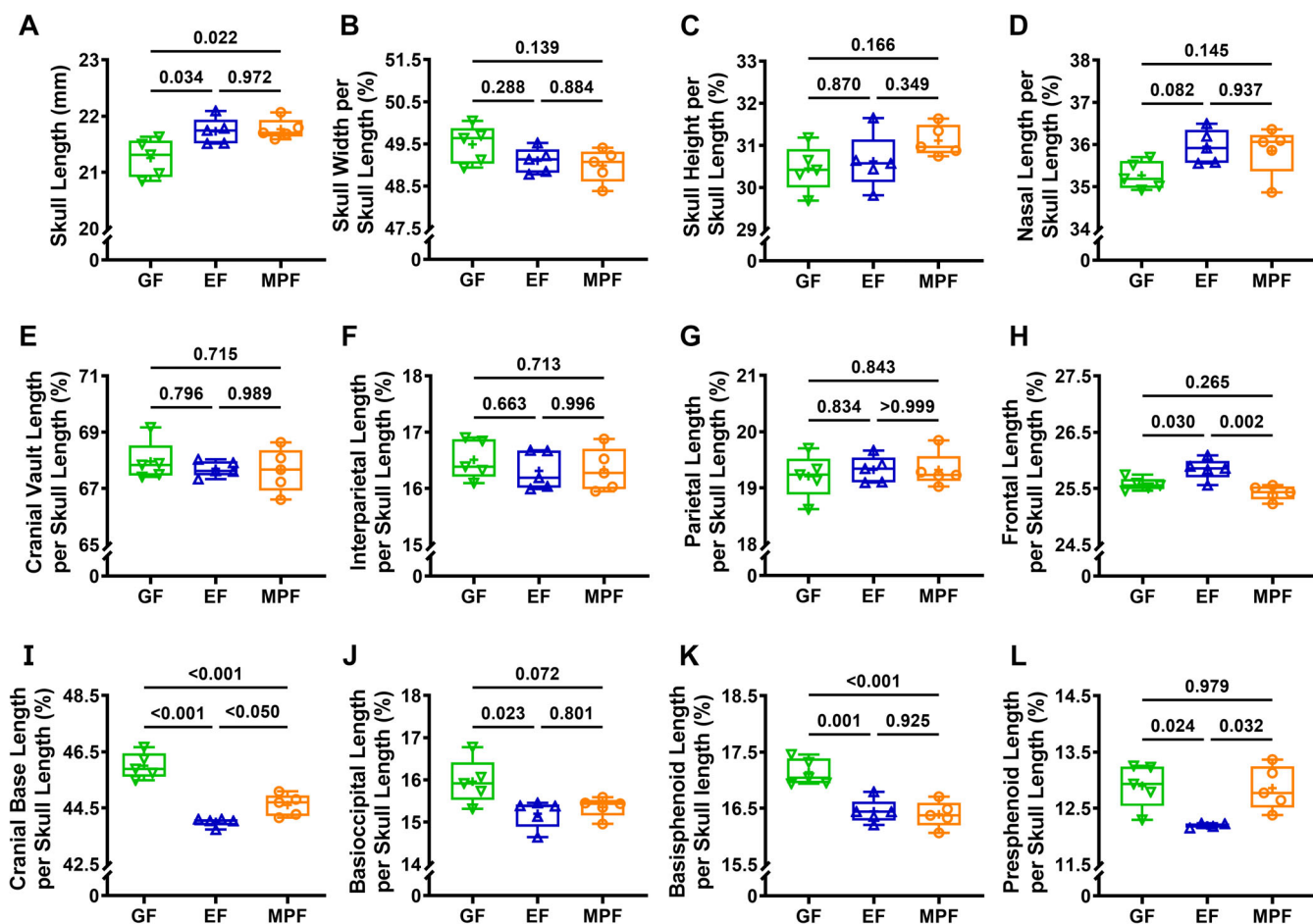


Fig. 2. Commensal microbiota impact craniofacial skeletal morphology in 9-week-old female C57BL/6T mice. Female C57BL/6T GF mice (no microbes), EF mice (commensal microbiota), and MPF mice (commensal microbiota with SFB) were euthanized at age 9 weeks; skulls were isolated for analyses ($n = 5$ /group). Craniometric measurements were performed using μ CT 3D reconstructions of the skull and standard craniometric landmarks (Fig. S1): skull length (A); skull width per skull length (B); skull height per skull length (C); nasal bone length per skull length (D); cranial vault length per skull length (E); interparietal bone length per skull length (F); parietal bone length per skull length (G); frontal bone length per skull length (H); cranial base length per skull length (I); basioccipital bone length per skull length (J); basisphenoid bone length per skull length (K); presphenoid bone length per skull length (L). One-way ANOVA ($\alpha = 0.05$) with Tukey post hoc test ($p < 0.05$) was carried out comparing outcomes in GF, EF, and MPF mice.

influence the skull length. The direct skull length was similar in MPF versus EF mice (Fig. 2A), which implies that commensal gut microbes do not contribute to skull length. Skull width per skull length (Fig. 2B), skull height per skull length (Fig. 2C), and nasal bone length per skull length (Fig. 2D) were not different in EF versus GF mice or MPF versus EF mice. These data support the idea that the commensal microbiota does not influence the relative skull width, skull height, or nasal bone length in 9-week-old female C57BL/6T mice.

Cranial vault bone length analyses (Fig. 2E–H) demonstrated that the cranial vault length per skull length was not different in EF versus GF mice or MPF versus EF mice (Fig. 2E). The similar relative cranial vault lengths found in EF versus GF mice and MPF versus EF mice (Fig. 2E) were attributed to a lack of alterations in interparietal (Fig. 2F) and parietal (Fig. 2G) bone lengths per skull length. Interestingly, the frontal bone length per skull length was increased in EF versus GF mice and reduced in MPF versus EF mice (Fig. 2H). The increased relative frontal bone length detected in EF versus GF mice (Fig. 2H) suggests that the

commensal microbiota affects cranial vault growth and morphology. The reduced relative frontal bone length detected in MPF versus EF mice (Fig. 2H) supports the idea that commensal gut microbes play a role in commensal microbiota effects on cranial vault growth and morphology.

Cranial base bone length analyses (Fig. 2I–L) showed the cranial base length per skull length was decreased in EF versus GF mice (Fig. 2I). The shortened relative cranial base length in EF versus GF mice (Fig. 2I) was attributed to EF mice having reduced basioccipital (Fig. 2J), basisphenoid (Fig. 2K), and presphenoid (Fig. 2L) bone lengths per skull length. Cranial base craniometric findings in EF versus GF mice suggest that the commensal microbiota influences cranial base growth and morphology. Cranial base analyses comparing MPF versus EF mice showed that MPF mice exhibited an increased cranial base length per skull length (Fig. 2I). The elongated relative cranial base length in MPF versus EF mice (Fig. 2I) was due to MPF mice having an enhanced presphenoid bone length per skull length (Fig. 2L). Cranial base craniometric study outcomes

in MPF versus EF mice support the idea that commensal gut microbes contribute to commensal microbiota effects on cranial base growth and morphology.

Commensal microbiota does not affect cranial bone mineral density in 9-week-old female C57BL/6T mice

We carried out BMD analyses in the reconstructed 3D μ CT images of skulls to elucidate commensal microbiota effects on bone mass in the cranial vault and cranial base. Cranial vault analyses included the interparietal, parietal, and frontal bones (Fig. S2A–D), and cranial base analyses included the basioccipital, basisphenoid, and presphenoid bones (Fig. S2E–H). Cranial vault BMD outcomes were not different in EF versus GF mice or MPF versus EF mice (Fig. S2A–D). Furthermore, cranial base BMD outcomes were similar in EF versus GF mice and MPF versus EF mice (Fig. S2E–H). BMD study findings support the idea that the commensal microbiota does not critically impact bone mass accrual in the cranial vault or cranial base of 9-week-old female C57BL/6T mice.

Discussion

This study comparing 9-week-old female C57BL/6T mice reared under defined barrier conditions revealed that the commensal microbiota plays a role in craniofacial skeletal growth and morphology. Results comparing GF mice to EF mice showed that the commensal microbiota can enlarge the gross skull length and restrict the relative cranial base length. Results comparing EF mice to MPF mice, which differ by SFB colonization status, demonstrated that MPF mice exhibited an elongated relative cranial base length. These findings support the idea that commensal gut microbes contribute to craniofacial skeletal growth and morphology.

Comparing GF mice to EF mice demonstrated that the commensal microbiota attenuated the relative cranial base length owing to decreased relative basioccipital, basisphenoid, and presphenoid bone lengths. Appreciating that cranial base bones form through endochondral ossification, these findings are in line with prior studies showing that the commensal microbiota regulates endochondral bone formation processes at nonoral skeletal sites.^[9–14] Interestingly, EF versus GF mice exhibited an increased relative length in the frontal bone. The frontal bone forms through intramembranous ossification, suggesting that commensal microbiota also influences intramembranous bone formation processes.

While this initial report was centered on craniometry, future studies should evaluate suture and synchondrosis involvement. This is important because sutures and synchondroses contribute to craniofacial skeletal growth and morphology. Moreover, studies are needed to further assess commensal microbiota effects on the cranial base. The cranial base plays an extremely important role in total skull morphology as the growth site for the skull is located at the ISS.^[48] The cranial base develops earlier than the face or cranial vault and has long been thought to provide patterning and instructions for the final form of the overall skull.^[49] Several studies have suggested that cranial base length can predict specific malocclusions in adult life.^[50] Additionally, alterations in the cranial base angle have been shown to cause skeletal malocclusions.^[51]

We investigated the 9-week-old time point because craniofacial skeletal growth peaks around postnatal day 60 in female C57BL/6T mice.^[21] Future investigations are needed to evaluate

earlier time points to define critical postnatal periods where the commensal microbiota contributes to craniofacial skeletal growth and morphology. We utilized μ CT to discern commensal microbiota effects on craniometric and BMD outcomes in the postnatal craniofacial skeleton. Ongoing studies are necessary that use histology to delineate cellular and molecular mechanisms mediating commensal microbiota actions on growth and morphology in the craniofacial skeletal complex.

Prior work by our group and others established that commensal microbiota effects on noncraniofacial bone growth and morphology were influenced by mouse strain genetic determinants. Whereas the commensal microbiota impairs bone mass accrual and microarchitecture in long bones of growing C57BL/6 mice,^[9, 10] the commensal microbiota promotes bone formation and longitudinal growth in long bones of growing BALB/c^[11] and CB6F1 mice.^[12] Study outcomes reported herein revealed that the commensal microbiota promoted gross skull length and restricted relative cranial base length in C57BL/6 mice. Future research is necessary to determine whether commensal microbiota effects on craniofacial skeletal growth and morphology differ across murine strains.

GF mice were fed LabDiet 5010, and specific-pathogen-free mice (EF, MPF mice) were fed NIH-31M diet. LabDiet 5010 and NIH-31M are standard hard pellet rodent diets, but they have minor differences in composition and may differ in hardness/consistency. Knowing that administering a soft versus hard diet can affect dentofacial growth outcomes,^[52, 53] a potential study design weakness is that GF and specific-pathogen-free mice were not administered the same diet. However, all experimental groups were fed a hard diet, so minor differences in diet consistency are not expected to influence outcomes as dramatically as if the groups were fed soft versus hard diets. Additionally, comparing EF versus MPF mice (both fed NIH-31M) demonstrated alterations in craniofacial skeletal outcomes, which supports the idea that commensal microbiota effects on craniofacial morphology are independent of diet. However, it will be important for future studies to utilize the same diet across GF and specific-pathogen-free animal groups to eliminate diet as a potentially confounding variable.

Investigations in GF animal models have demonstrated that the commensal microbiota supports normal brain development and behavior.^[54–57] The growth of the brain, which is housed in the skull, is a major determinant of craniofacial growth and morphology.^[58–62] Therefore, commensal microbiota actions supporting normal brain development could contribute to the growth and morphology of the craniofacial skeleton through an increase in cranial capacity. This highlights the need for future research elucidating whether commensal microbiota regulation of brain development plays a role in commensal microbiota actions on craniofacial skeletal growth and morphology.

This investigation comparing MPF versus EF mice, which differ by SFB colonization status, supports the idea that commensal gut microbes play a role in the growth and morphology of the craniofacial skeleton. SFB is a commensal gut bacterium that colonizes the ileum after weaning.^[25–27] SFB colonization has broad innate and adaptive immunostimulatory effects, including the induction of $T_H17/IL17A$ -mediated immunity.^[27, 28, 63–66] We and others have shown that SFB contributes to commensal microbiota actions on skeletal growth and maturation at noncraniofacial sites. SFB induction of $T_H17/IL17A$ -mediated immunity promoted bone-resorbing osteoclasts and impaired trabecular bone morphology in the long bones of growing mice.^[13, 14] Further, prior reports linked SFB induction of $T_H17/IL17A$ immunity

to commensal microbiota actions in neurodevelopmental abnormalities.^[29, 30] Therefore, commensal gut microbe contributions to craniofacial skeletal growth and morphology could be mediated through multifactorial effects on bone cell actions and brain development.

While SFB has been shown to colonize humans and upregulate T_H17 cell immune pathway genes,^[67–69] *Bifidobacterium adolescentis* is another commensal gut bacterium that has been linked to the clinical induction of T_H17/IL17A-mediated immunity.^[70] Dietary modification^[71, 72] and probiotic administration^[73, 74] impact SFB colonization status, which implies that noninvasive interventions in the commensal gut microbiota could be employed to modify craniofacial skeletal growth and morphology. While randomized controlled clinical trials have shown that probiotics have protective effects on the aging skeleton and brain,^[75, 76] future investigations are needed to show whether probiotics could be employed to direct craniofacial skeletal growth and morphology.

Our study comparing EF versus MPF mice, which differ by a known commensal gut bacterium, supports the premise that commensal gut microbes play a role in craniofacial development. However, future research is necessary to further determine how specific microbiota communities (i.e., oral, gut) contribute to craniofacial skeletal morphology. Conventionalized animal studies, in which GF animals are associated/colonized with oral microbiota versus gut microbiota from specific-pathogen-free mice, would delineate how different microbiota communities contribute to craniofacial skeletal growth and maturation.

Author Contributions

Joy E. Gerasco: Conceptualization; data curation; formal analysis; funding acquisition; investigation; methodology; software; writing – original draft; writing – review and editing. **Jessica D. Hathaway-Schrader:** Data curation; formal analysis; investigation; writing – review and editing. **Nicole A. Poulides:** Data curation; investigation; writing – review and editing. **Matthew D. Carson:** Data curation; formal analysis; investigation; writing – review and editing. **Naoto Okhura:** Methodology; writing – review and editing. **Caroline Westwater:** Conceptualization; investigation; methodology; writing – review and editing. **Nan E Hatch:** Conceptualization; methodology; supervision; writing – review and editing. **Chad M. Novince:** Conceptualization; formal analysis; funding acquisition; investigation; methodology; resources; software; supervision; writing – original draft; writing – review and editing.

Funding Information

This work was funded by an American Society for Bone and Mineral Research Rising Star Award, K08DE025337, T32DE017551, P20GM130457, P30DK123704, P20GM121342, R01DE029637, R01AG067510, UL1TR001450, F30DE027290, R01AR081488.

Disclosures

The authors declare no conflicts of interest.

Peer Review

The peer review history for this article is available at <https://www.webofscience.com/api/gateway/wos/peer-review/10.1002/jbm4.10775>.

Data Availability Statement

The data used and/or analyzed during the current study are available from the corresponding author upon request.

References

1. Belkaid Y, Naik S. Compartmentalized and systemic control of tissue immunity by commensals. *Nat Immunol*. 2013;14(7):646–653.
2. Brestoff JR, Artis D. Commensal bacteria at the interface of host metabolism and the immune system. *Nat Immunol*. 2013;14(7):676–684.
3. Thaiss CA, Zmora N, Levy M, Elinav E. The microbiome and innate immunity. *Nature*. 2016;535(7610):65–74.
4. Zheng D, Liwinski T, Elinav E. Interaction between microbiota and immunity in health and disease. *Cell Res*. 2020;30(6):492–506.
5. Sommer F, Backhed F. The gut microbiota—masters of host development and physiology. *Nat Rev Microbiol*. 2013;11(4):227–238.
6. Schroeder BO, Backhed F. Signals from the gut microbiota to distant organs in physiology and disease. *Nat Med*. 2016;22(10):1079–1089.
7. Krautkramer KA, Fan J, Backhed F. Gut microbial metabolites as multi-kingdom intermediates. *Nat Rev Microbiol*. 2021;19(2):77–94.
8. Fan Y, Pedersen O. Gut microbiota in human metabolic health and disease. *Nat Rev Microbiol*. 2021;19(1):55–71.
9. Sjögren K, Engdahl C, Henning P, et al. The gut microbiota regulates bone mass in mice. *J Bone Miner Res*. 2012;27(6):1357–1367.
10. Novince CM, Whittow CR, Aartun JD, et al. Commensal gut microbiota immunomodulatory actions in bone marrow and liver have catabolic effects on skeletal homeostasis in health. *Sci Rep*. 2017;7(1):5747.
11. Schwarzer M, Makki K, Storelli G, et al. *Lactobacillus plantarum* strain maintains growth of infant mice during chronic undernutrition. *Science*. 2016;351(6275):854–857.
12. Yan J, Herzog JW, Tsang K, et al. Gut microbiota induce IGF-1 and promote bone formation and growth. *Proc Natl Acad Sci U.S.A.* 2016; 113(47):E7554–E7563.
13. Hathaway-Schrader JD, Poulides NA, Carson MD, et al. Specific commensal bacterium critically regulates gut microbiota osteoimmunomodulatory actions during normal postpubertal skeletal growth and maturation. *JBM R Plus*. 2020;4(3):e10338.
14. Tyagi AM, Darby TM, Hsu E, et al. The gut microbiota is a transmissible determinant of skeletal maturation. *Elife*. 2021;10:e64237.
15. Galea GL, Zein MR, Allen S, Francis-West P. Making and shaping endochondral and intramembranous bones. *Dev Dyn*. 2021;250(3):414–449.
16. White HE, Goswami A, Tucker AS. The intertwined evolution and development of sutures and cranial morphology. *Front Cell Dev Biol*. 2021;9:653579.
17. Lacruz RS, Stringer CB, Kimbel WH, et al. The evolutionary history of the human face. *Nat Ecol Evol*. 2019;3(5):726–736.
18. Park KM, Tripathi NV, Mufarrej FA. Quality of life in patients with craniosynostosis and deformational plagiocephaly: a systematic review. *Int J Pediatr Otorhinolaryngol*. 2021;149:110873.
19. Kawakami M, Yamamura K. Cranial bone morphometric study among mouse strains. *BMC Evol Biol*. 2008;8:73.
20. Vora SR, Camci ED, Cox TC. Postnatal ontogeny of the cranial base and craniofacial skeleton in male C57BL/6J mice: a reference standard for quantitative analysis. *Front Physiol*. 2015;6:417.
21. Wei X, Thomas N, Hatch NE, Hu M, Liu F. Postnatal craniofacial skeletal development of female C57BL/6Ncr1 mice. *Front Physiol*. 2017;8:697.

22. Young DL, Schneider RA, Hu D, Helms JA. Genetic and teratogenic approaches to craniofacial development. *Crit Rev Oral Biol Med*. 2000;11(3):304–317.
23. Neben CL, Merrill AE. Signaling pathways in craniofacial development: insights from rare skeletal disorders. *Curr Top Dev Biol*. 2015; 115:493–542.
24. Stanton E, Urata M, Chen JF, Chai Y. The clinical manifestations, molecular mechanisms and treatment of craniosynostosis. *Dis Model Mech*. 2022;15(4):1–18.
25. Klaasen HL, Koopman JP, Beynen AC. Effects of age, strain and social hierarchy on colonization of autochthonous, segmented, filamentous bacteria in the ileum of mice. *Microecol Therapy*. 1990b;20: 17–20.
26. Snel J, Hermsen CC, Smits HJ, et al. Interactions between gut-associated lymphoid tissue and colonization levels of indigenous, segmented, filamentous bacteria in the small intestine of mice. *Can J Microbiol*. 1998;44(12):1177–1182.
27. Gaboriau-Routhiau V, Rakotobe S, Lecuyer E, et al. The key role of segmented filamentous bacteria in the coordinated maturation of gut helper T cell responses. *Immunity*. 2009;31(4):677–689.
28. Ivanov II, Atarashi K, Manel N, et al. Induction of intestinal Th17 cells by segmented filamentous bacteria. *Cell*. 2009;139(3):485–498.
29. Kim S, Kim H, Yim YS, et al. Maternal gut bacteria promote neurodevelopmental abnormalities in mouse offspring. *Nature*. 2017; 549(7673):528–532.
30. Lammert CR, Frost EL, Bolte AC, et al. Cutting edge: critical roles for microbiota-mediated regulation of the immune system in a prenatal immune activation model of autism. *J Immunol*. 2018;201(3): 845–850.
31. Massimi L, Bianchi F, Frassanito P, Calandrelli R, Tamburrini G, Caldarelli M. Imaging in craniosynostosis: when and what? *Childs Nerv Syst*. 2019;35(11):2055–2069.
32. Dot G, Rafflenbeul F, Arbotto M, Gajny L, Rouch P, Schouman T. Accuracy and reliability of automatic three-dimensional cephalometric landmarking. *Int J Oral Maxillofac Surg*. 2020;49(10):1367–1378.
33. Council NR. *Guide for the care and use of laboratory animals*. Eighth ed. Washington, DC: The National Academies Press; 2011.
34. Bacchetti De Gregoris T, Aldred N, Clare AS, Burgess JG. Improvement of phylum- and class-specific primers for real-time PCR quantification of bacterial taxa. *J Microbiol Methods*. 2011;86(3):351–356.
35. Hathaway-Schrader JD, Steinkamp HM, Chavez MB, et al. Antibiotic perturbation of gut microbiota dysregulates osteoimmune cross talk in postpubertal skeletal development. *Am J Pathol*. 2019;189(2): 370–390.
36. Swanson BA, Carson MD, Hathaway-Schrader JD, et al. Antimicrobial-induced oral dysbiosis exacerbates naturally occurring alveolar bone loss. *FASEB J*. 2021;35(11):e22015.
37. Packey CD, Shanahan MT, Manick S, et al. Molecular detection of bacterial contamination in gnotobiotic rodent units. *Gut Microbes*. 2013; 4(5):361–370.
38. Hathaway-Schrader JD, Aartun JD, Poulides NA, et al. Commensal oral microbiota induces osteoimmunomodulatory effects separate from systemic microbiome in mice. *JCI Insight*. 2022;7(4):1–20.
39. Livak KJ, Schmittgen TD. Analysis of relative gene expression data using real-time quantitative PCR and the 2(-Delta Delta C(T)) method. *Methods*. 2001;25(4):402–408.
40. Schmittgen TD, Livak KJ. Analyzing real-time PCR data by the comparative C(T) method. *Nat Protoc*. 2008;3(6):1101–1108.
41. Hathaway-Schrader JD, Carson MD, Gerasco JE, et al. Commensal gut bacterium critically regulates alveolar bone homeostasis. *Lab Invest*. 2022;102(4):363–375.
42. Liu J, Nam HK, Campbell C, Gasque KC, Millán JL, Hatch NE. Tissue-nonspecific alkaline phosphatase deficiency causes abnormal craniofacial bone development in the *Alpl*(–/–) mouse model of infantile hypophosphatasia. *Bone*. 2014;67:81–94.
43. Xu H, Lenhart SA, Chu EY, et al. Dental and craniofacial defects in the *Crtap*(–/–) mouse model of osteogenesis imperfecta type VII. *Dev Dyn*. 2020;249(7):884–897.
44. Nam HK, Emmanouil E, Hatch NE. Deletion of the pyrophosphate generating enzyme ENPP1 rescues craniofacial abnormalities in the *TNAP*(–/–) mouse model of Hypophosphatasia and reveals FGF23 as a marker of phenotype severity. *Front Dent Med*. 2022;3:1–14.
45. Bouxsein ML, Boyd SK, Christiansen BA, Guldberg RE, Jepsen KJ, Müller R. Guidelines for assessment of bone microstructure in rodents using micro-computed tomography. *J Bone Miner Res*. 2010;25(7):1468–1486.
46. Liu J, Nam HK, Wang E, Hatch NE. Further analysis of the Crouzon mouse: effects of the *FGFR2*(C342Y) mutation are cranial bone-dependent. *Calcif Tissue Int*. 2013;92(5):451–466.
47. Liu J, Campbell C, Nam HK, et al. Enzyme replacement for craniofacial skeletal defects and craniosynostosis in murine hypophosphatasia. *Bone*. 2015;78:203–211.
48. Funato N. New insights into cranial synchondrosis development: a mini review. *Front Cell Dev Biol*. 2020;8:706.
49. Bastir M. Craniofacial levels and the morphological maturation of the human skull. *J Anat*. 2006;209:637–654.
50. Gong A, Li J, Wang Z, et al. Cranial base characteristics in anteroposterior malocclusions: a meta-analysis. *Angle Orthod*. 2016;86(4): 668–680.
51. Almeida KCM, Raveli TB, Vieira CIV, Santos-Pinto AD, Raveli DB. Influence of the cranial base flexion on class I, II and III malocclusions: a systematic review. *Dental Press J Orthod*. 2017;22(5):56–66.
52. Kiliaridis S. The importance of masticatory muscle function in dento-facial growth. *Semin Orthod*. 2006;12(2):110–119.
53. Kono K, Tanikawa C, Murata Y, Yanagita T, Kamioka H, Yamashiro T. Three-dimensional changes in the craniofacial complex associated with soft-diet feeding. *Eur J Orthod*. 2020;42(5):509–516.
54. Heijtz RD, Wang S, Anuar F, et al. Normal gut microbiota modulates brain development and behavior. *Proc Natl Acad Sci U.S.A.* 2011; 108(7):3047–3052.
55. Hoban AE, Stilling RM, Ryan FJ, et al. Regulation of prefrontal cortex myelination by the microbiota. *Transl Psychiatry*. 2016;6(4):e774.
56. Lu J, Synowiec S, Lu L, et al. Microbiota influence the development of the brain and behaviors in C57BL/6J mice. *PLoS One*. 2018;13(8): e0201829.
57. Ahmed S, Travis SD, Díaz-Bahamonde FV, et al. Early influences of microbiota on white matter development in germ-free piglets. *Front Cell Neurosci*. 2021;15:807170.
58. Moss ML, Young RW. A functional approach to craniology. *Am J Phys Anthropol*. 1960;18(4):281–292.
59. Lieberman DE, Pearson OM, Mowbray KM. Basicranial influence on overall cranial shape. *J Hum Evol*. 2000;38(2):291–315.
60. Hallgrímsson B, Lieberman DE. Mouse models and the evolutionary developmental biology of the skull. *Integr Comp Biol*. 2008;48(3): 373–384.
61. Marcucio RS, Young NM, Hu D, Hallgrímsson B. Mechanisms that underlie co-variation of the brain and face. *Genesis*. 2011;49(4): 177–189.
62. Adameyko I, Fried K. The nervous system orchestrates and integrates craniofacial development: a review. *Front Physiol*. 2016;7:49.
63. Goto Y, Panea C, Nakato G, et al. Segmented filamentous bacteria antigens presented by intestinal dendritic cells drive mucosal Th17 cell differentiation. *Immunity*. 2014;40(4):594–607.
64. Lecuyer E, Rakotobe S, Lengline-Garnier H, et al. Segmented filamentous bacterium uses secondary and tertiary lymphoid tissues to induce gut IgA and specific T helper 17 cell responses. *Immunity*. 2014;40(4):608–620.
65. Panea C, Farkas AM, Goto Y, et al. Intestinal monocyte-derived macrophages control commensal-specific Th17 responses. *Cell Rep*. 2015;12(8):1314–1324.
66. Flannigan KL, Ngo VL, Geem D, et al. IL-17A-mediated neutrophil recruitment limits expansion of segmented filamentous bacteria. *Mucosal Immunol*. 2017;10(3):673–684.
67. Yin Y, Wang Y, Zhu L, et al. Comparative analysis of the distribution of segmented filamentous bacteria in humans, mice and chickens. *ISME J*. 2013;7(3):615–621.

68. Chen B, Chen H, Shu X, et al. Presence of segmented filamentous bacteria in human children and its potential role in the modulation of human gut immunity. *Front Microbiol.* 2018;9:1403.
69. Chen H, Wang L, Wang X, Wang X, Liu H, Yin Y. Distribution and strain diversity of Immunoregulating segmented filamentous bacteria in human intestinal lavage samples. *Microb Ecol.* 2020;79(4):1021–1033.
70. Tan TG, Sefik E, Geva-Zatorsky N, et al. Identifying species of symbiont bacteria from the human gut that, alone, can induce intestinal Th17 cells in mice. *Proc Natl Acad Sci U.S.A.* 2016;113(50):E8141–E8150.
71. Koopman JP, van den Brink ME, Scholten PM. Further studies with the segmented filamentous intestinal bacteria of mice; effects of physical and chemical factors on survival and the effects of milk diet, para-aminobenzoic acid and mouse strain on colonization. *Zeitschrift fur Versuchstierkunde.* 1988;31(6):270–275.
72. Koopman JP, van den Brink ME, Scholtenl PM, et al. The influence of stress and cheese-whey on intestinal parameters in mice. *Vet Q.* 1989; 11(1):24–29.
73. Fuentes S, Egert M, Jimenez-Valera M, Monteoliva-Sanchez M, Ruiz-Bravo A, Smidt H. A strain of *Lactobacillus plantarum* affects segmented filamentous bacteria in the intestine of immunosuppressed mice. *FEMS Microbiol Ecol.* 2008;63(1):65–72.
74. Liao N, Yin Y, Sun G, et al. Colonization and distribution of segmented filamentous bacteria (SFB) in chicken gastrointestinal tract and their relationship with host immunity. *FEMS Microbiol Ecol.* 2012;81(2): 395–406.
75. Nilsson AG, Sundh D, Bäckhed F, Lorentzon M. *Lactobacillus reuteri* reduces bone loss in older women with low bone mineral density: a randomized, placebo-controlled, double-blind, clinical trial. *J Intern Med.* 2018;284(3):307–317.
76. Kim CS, Cha L, Sim M, et al. Probiotic supplementation improves cognitive function and mood with changes in gut microbiota in community-dwelling older adults: a randomized, double-blind, placebo-controlled, multicenter trial. *J Gerontol A Biol Sci Med Sci.* 2021;76(1):32–40.